

Association and Thermal Gelation in Aqueous Mixtures of Ethyl(hydroxyethyl)cellulose and Ionic Surfactant: FTIR and Raman Study

D. Ostrovskii,^{*,†} A.-L. Kjøniksen,[‡] B. Nyström,[‡] and L. M. Torell[†]

Department of Experimental Physics, Chalmers University of Technology, SE-41296 Göteborg, Sweden, and Department of Chemistry, University of Oslo, P.O. Box 1033, Blindern, N-0315 Oslo, Norway

Received September 9, 1998; Revised Manuscript Received December 10, 1998

ABSTRACT: The first attempt to investigate polymer–surfactant interactions in gelling and nongelling aqueous mixtures of a nonionic cellulose ether and a surfactant by means of vibrational spectroscopy is presented. A series of aqueous solutions of ethyl(hydroxyethyl)cellulose (EHEC) with addition of anionic surfactant sodium dodecyl sulfate (SDS) of different concentrations was thoroughly investigated by means of Raman scattering and FTIR absorption techniques. Our data show that even in the sol state (i.e., below the gel point) there are interactions between the polymer and the surfactant, and both bound and free surfactant molecules were detected. This interaction, which cannot be characterized as a chemical one, occurs mainly between the side chains of the polymer and the sulfonic acid groups of SDS. Above the gel point, a new type of interaction appears, which mainly involves the SO_3^- groups and water molecules. The intermolecular interactions are studied vs changes of both temperature and polymer–surfactant compositions, and a possible model for the gelation process is discussed.

Introduction

Originally, the problem of interactions between polymers and surfactants has arisen from the studies of biological systems^{1,2} such as proteins and natural lipids. In recent years, systems formed by hydrophobically modified water-soluble polymers and surfactants have gained special attention because of their growing importance for a wide range of technical applications (pharmaceuticals, paints, oil recovery, etc.).^{3–6} A typical example of this class of systems is the aqueous mixture of ethyl(hydroxyethyl)cellulose (EHEC) and the anionic surfactant sodium dodecyl sulfate (SDS). In the presence of moderate surfactant concentrations, this system forms a transparent thermoreversible gel in the semidilute polymer concentration regime at elevated temperatures.^{7–9} Different physical properties of EHEC–surfactant systems have been studied by a large variety of experimental techniques.^{7–19} NMR self-diffusion experiments revealed⁹ that there is, even in the solution state, a significant interaction between the polymer and the surfactant. Moreover, it was shown that the degree of surfactant binding to the polymer is independent of temperature when the sol transforms to a gel. It was found¹⁷ that the gelation process is governed by a delicate interplay between swelling and associative properties of the system. The general picture that emerged^{15,16} was that the gel formation is governed by factors such as the type of EHEC sample, polymer concentration, level and type of added surfactant, salinity, and temperature. In this context we may note that there are several theoretical investigations aimed to describe the mechanisms of thermoreversible gelation in solutions of associating polymers.^{20–22}

Most of the previous studies of the EHEC–surfactant interactions were dealing with macroscopic aspects of

the systems, and little is known concerning the behavior on the molecular level. Vibrational spectroscopy constitutes a powerful method to explore the local properties of the systems. A possible reason for the lack of spectroscopic investigations on gelling EHEC–surfactant systems may be the fairly low concentrations of both polymer and surfactant at which the interesting properties occur. Such conditions make it usually difficult to record high-quality IR and Raman spectra: long integrations time and repeated scans in the Raman measurements are needed, while in the infrared absorption experiments the thickness of the sample (which is proportional to the absorption intensity) is restricted by the absorption of water. Nevertheless, we have made an attempt to use vibrational spectroscopy to study low-concentration EHEC/SDS/water systems. The aim of the work is to obtain information, on a local scale, about the molecular interactions to gain further insight into the nature of thermoreversible gelation.

In the present work we will report results from a Raman/FTIR absorption study on aqueous systems of EHEC/SDS of various compositions (some characteristic features of the systems are given in Table 1) and at different temperatures, representing both the sol and the gel states.

Experimental Section

Samples. The EHEC sample, designated Bermocoll DVT 89017, was manufactured by Akzo Nobel Surface Chemistry AB, Stenungsund, Sweden. The degree of substitution of ethyl groups was $\text{DS}_{\text{ethyl}} = 1.9$ per anhydroglucose unit, and the molar substitution of the ethylene oxide groups was $\text{MS}_{\text{EO}} = 1.3$ per anhydroglucose unit. The number-average molecular weight of this polydisperse sample ($M_w/M_n \approx 2$) is approximately 80 000. All the above data were given by the manufacturer. The surfactant SDS was obtained from Fluka and was used as received. The detailed procedure of the EHEC sample preparation and the preparation of homogeneous solutions have been described elsewhere.⁹ The main characteristics of the samples studied in this work are listed in Table 1.

* Corresponding author. Tel +46-31-772-8038; fax +46-31-772-3177; e-mail dostr@fy.chalmers.se.

[†] Chalmers University of Technology.

[‡] University of Oslo.

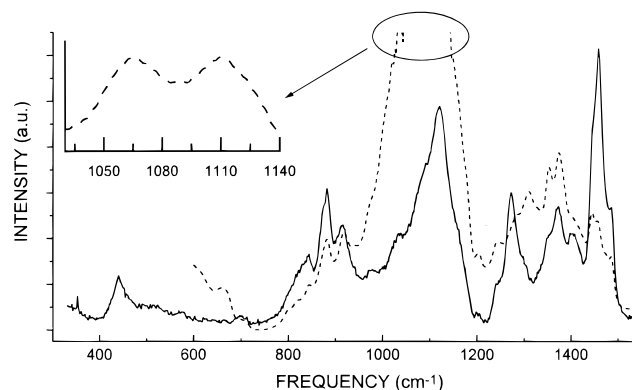


Figure 1. IR absorption (---) and Raman (—) spectra of solid EHEC at room temperature.

Table 1. Characteristics of the Present EHEC–SDS–Water Systems

sample	[EHEC] (wt %)	[SDS] (mM)	gel point (0 °C)
A	1	0	no gel
B	1	4	37
C	2	0	no gel
D	2	4	34
E	2	6	41
F	2	8	39
G	4	0	no gel
H	4	4	31
I	4	6	34
J	4	8	36
K	4	10	39
L	4	20	40

Experimental Setups. Raman spectra were recorded with a Spex double monochromator (model 1403, 1800 lines/mm holographic gratings) equipped with a C31034 photomultiplier. The spectral resolution was about 2.5 cm^{-1} . The 488 nm band of Ar ion laser (Spectra-Physics 2020) was used as an excitation source. During the measurements the solutions were placed in a sealed glass cuvette with optical windows such that the path length of the laser beam through the sample was about 15 mm. Each spectrum presented below was obtained as a result of averaging of at least 50 scans.

Infrared absorption measurements were made with Bruker 22 (Vektor) FTIR spectrometer. A standard liquid cell (Crystran Ltd) with polished ZnSe windows, and a path length of $25\text{ }\mu\text{m}$ was used.

Temperature Measurements. It should be noted that for the same state of the sample (solution or gel) we observed, within the accuracy of the measurements, no obvious differences between the spectra taken at different temperatures (for example, 10 and $25\text{ }^{\circ}\text{C}$ or 45 and $70\text{ }^{\circ}\text{C}$, respectively). Therefore, we recorded the spectra without trying to be at the exact gelation temperature of the considered sample. However, to avoid phase separation of the samples¹⁵ during the Raman experiments, great care was exercised to set the heating rate such that the gels were transparent all the time (no signs of turbidity). By this measure of precaution, we can claim that all the Raman spectra were recorded for non-phase-separated systems. In the case of the FTIR measurements it was not possible to visually inspect the state of the sample. However, taking into account that the temperature of the cell was not higher than $45\text{ }^{\circ}\text{C}$, and also the geometry of the sample cell (path length of $25\text{ }\mu\text{m}$), we are quite sure that all the spectra were taken from samples that had not phase separated.

Results and Discussion

Pure Initial Components. Figure 1 shows the Raman and IR spectra of the pure solid ethyl(hydroxy-ethyl)cellulose. It should be noted that, among the large number of spectroscopic investigations carried out on unmodified or modified cellulose and different poly-

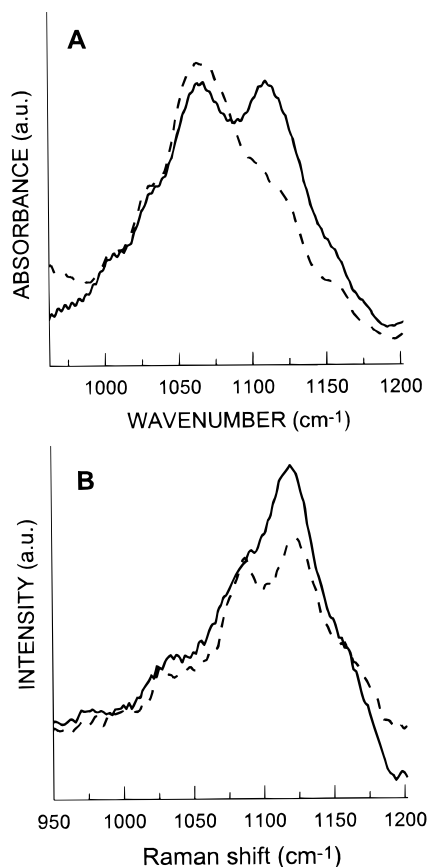


Figure 2. Comparison of room-temperature IR (A) and Raman (B) spectra of solid EHEC (—) and its aqueous solution (---).

saccharides,^{23–31} we found no study devoted to EHEC. Therefore, the band assignments made in the present article are based on reported for the cellulose and some of its derivatives.^{23–31} We furthermore note that the vibrational spectrum of any cellulose-based compound is quite complicated and that the simplest structural unit of cellulose (two pyranose cycles connected with C–O–C link) offers as much as 122 nonzero frequencies.²³ However, because of strong overlapping of the spectral bands (especially at room temperature), the number of experimentally observed bands is essentially smaller,²⁷ and the band assignment concerns mostly different spectral regions. Thus, the frequency interval between 300 and 900 cm^{-1} in Figure 1 is characteristic for the different ring vibrations,²⁵ whereas the range $1200\text{--}1500\text{ cm}^{-1}$ corresponds to the internal deformational vibrations of CH, CH_2 , and COH groups.^{28,29} The spectral region $700\text{--}950\text{ cm}^{-1}$ in Figure 1 may also reflect peculiarities of the monomer link structure and is sensitive to the distortions of the pyranose cycle conformation, as was shown both experimentally and theoretically.^{24,30}

It is well-known²⁶ that both the crystalline structure and the physical properties of any cellulose-based compound are affected to a large extent by the state of the hydrogen bonds. Figure 2 depicts the most important changes in the vibrational spectra of EHEC when the polymer is dissolved in water, and it is clearly seen from both the IR and the Raman spectra that the band around 1120 cm^{-1} decreases as the polymer dissolved. This band mainly includes contributions from the stretching vibrations (both symmetric and asymmetric) of the C–O–C bridges between neighboring pyranose

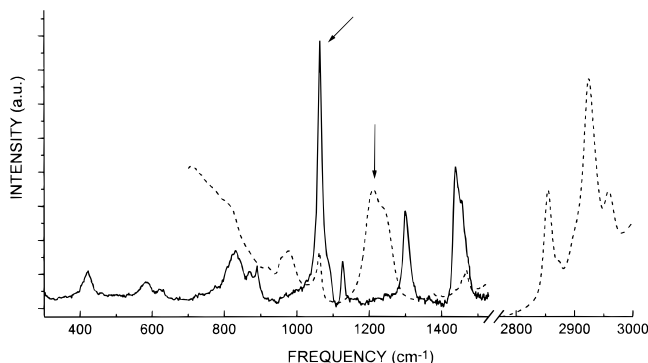


Figure 3. IR absorption (---) and Raman (—) spectra of SDS aqueous solution at room temperature. Arrows mark the bands corresponding to the SO_3^- stretching vibration (symmetrical in Raman, antisymmetrical in IR).

cycles (so-called glucosidic links).^{23,25,26} In the dissolved state the inter- and intramolecular hydrogen bonds are broken, and as a result, all glucose rings become more mobile and can move in different planes. Such a random (chaotic) motion of the rings will, in turn, strongly affect the “state” of the C–O–C bridges and hinder the stretching vibrations of the ring. Thus, the intensity of the discussed band around 1120 cm^{-1} can be used as a measure of the rigidity of the system (similar to the degree of crystallinity).

Figure 3 presents the IR and Raman spectra of SDS solution in water (salt concentration about 0.01 mol %). The most characteristic band is marked with an arrow, corresponding to the stretching vibration of the SO_3^- groups (of symmetric character in Raman whereas asymmetric in IR), and in this work used as a “finger-print” of SDS. The other spectral bands of SDS in Figure 3 are evidence of different types of C–C and C–H vibrations of the 1-dodecene.³¹ We will not consider these bands in the following, because they overlap with the EHEC bands of similar origin, and the low SDS concentration makes it practically impossible to carry out any precise analysis of their contribution.

EHEC–SDS Interaction at Room Temperature.

The addition of SDS to the aqueous EHEC solution causes several specific changes in the EHEC spectra. Figure 4 shows the IR absorption spectra of the EHEC/SDS/water systems at a constant EHEC concentration (4 wt %) and for different levels of SDS addition. It is immediately seen that with increasing SDS addition there are almost no transformations observed in the spectral region $1000\text{--}1180\text{ cm}^{-1}$, corresponding to the different glucosidic ring vibrations,^{23,26} whereas in the range between 1180 and 1330 cm^{-1} we note some characteristic changes (see inset in Figure 4). A new band centered at 1210 cm^{-1} appears in the spectrum as the surfactant concentration increases, and moreover, the intensity of the band at about 1250 cm^{-1} rises. Both the latter features can be ascribed as evidence of vibrations of the SO_3 groups in SDS (see Figure 3). In the frequency region $1280\text{--}1330\text{ cm}^{-1}$ the weak and broad absorption band, corresponding to the wagging and twisting vibrations of CH_2 groups of the EHEC,^{23,25} vanishes with surfactant addition. At the same time, the bands of the CH_2 bending vibrations (at about 1350 and 1375 cm^{-1}) are practically unchanged. The same behavior was also observed for samples with lower EHEC concentration (samples C–D–E–F, see Table 1) and may be explained by a decrease of the CH_2 mobility; i.e., the CH_2 groups become more fixed with surfactant addition. From the character of the CH_2 band transformation (the decrease of those bands corresponding to the vibrations of the only whole groups), we conclude that the interactions in the system are rather weak and cannot be attributed to chemical interactions. The finding agrees well with the previously reported conclusions^{16,17} that the polymer–surfactant interactions are governed by electrostatic and hydrophobic interactions.

Figure 5 shows the Raman spectra of the samples with no SDS (G) and with 20 mM SDS (L). The spectrum of pure SDS is also included for comparison. It is seen that the main spectral changes occurring with surfactant addition are the contributions of the SDS bands.

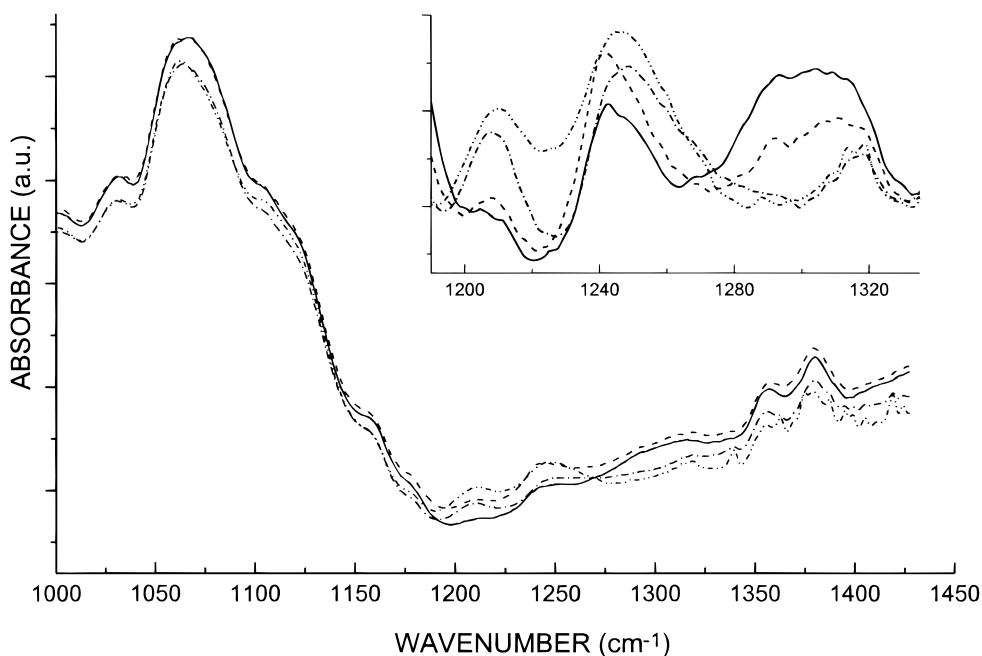


Figure 4. IR absorption spectra of EHEC aqueous solutions (4 wt %) with different SDS concentrations (at room temperature): (—) no SDS; (---) 4 mmol; (- · -) 10 mmol; (- - -) 20 mmol.

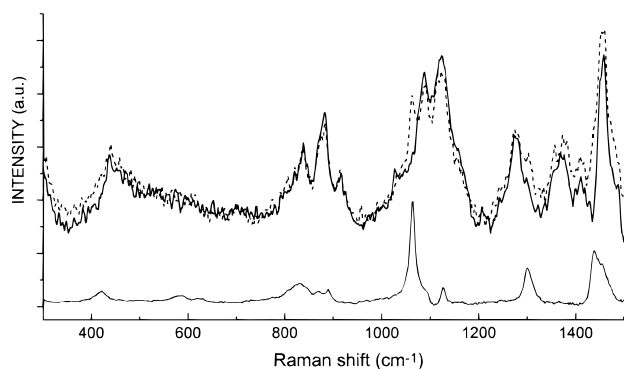


Figure 5. Raman spectra of 4 wt % EHEC aqueous solutions without (—) and with 20 mmol (---) SDS. The spectrum of SDS aqueous solution (bottom curve) is included for comparison.

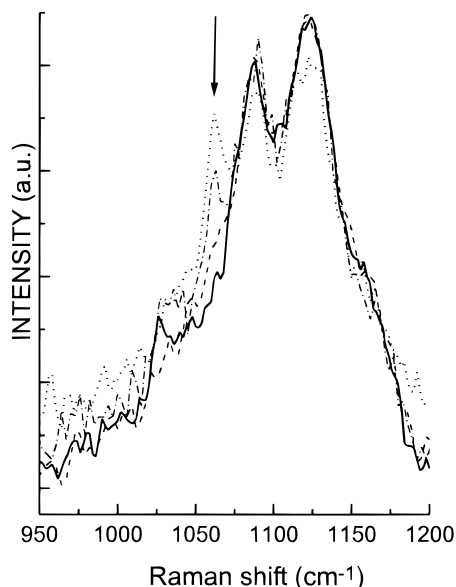


Figure 6. Raman spectra of 4 wt % EHEC aqueous solutions with different SDS concentrations: (—) no SDS; (- - -) 4 mmol; (- · - ·) 10 mmol; (- · · -) 20 mmol. Arrow marks the band of SO_3^- symmetrical stretching vibration.

It is important to stress that the unshifted frequency position of the SO_3^- symmetrical stretch (at 1060 cm^{-1}) explicitly shows that at room temperature in the EHEC–SDS system there are still SO_3^- groups in the “dissolved” state; i.e., they only interact with water molecules. It should be noted that “dissolved” SO_3^- groups are observed in the spectra even when the amount of SDS is low (4 mmol), and the intensity of the band gradually increasing as the SDS concentration increases (see Figure 6). However, curve-fitting procedures carried out for the G, H, K, and L samples in the frequency envelope $1000\text{--}1200\text{ cm}^{-1}$ (presented in Figure 6) show that the increase of the relative intensity of the discussed band is not a linear function of the SDS concentration. The last finding is consistent with that reported from a previous self-diffusion NMR study,⁹ where it was found that both the bound and free SDS fractions rise with surfactant concentration. In the cited NMR study it was also argued that the surfactant self-diffusion experiments revealed strong SDS–EHEC interactions, which apparently is in conflict with the statement above that the interaction in the systems are rather weak. However, the NMR results presented in ref 9 do not allow to decide whether the polymer–surfactant interaction is strong or not, but they merely

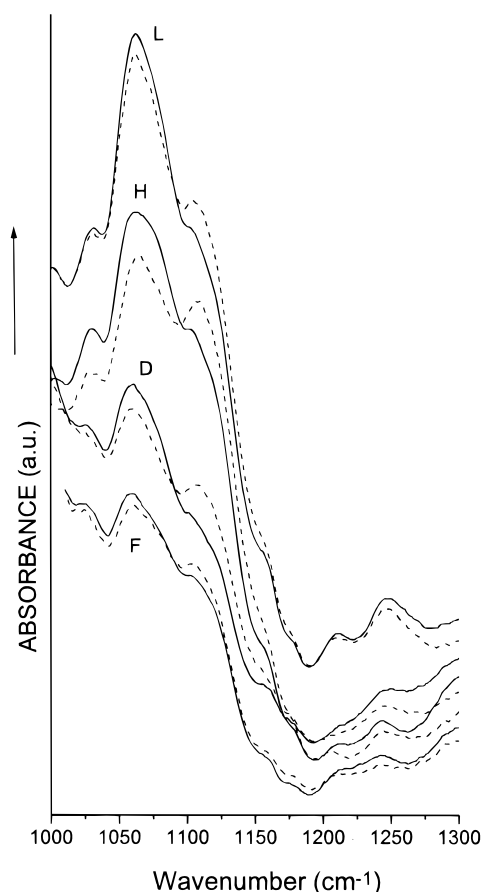


Figure 7. IR spectra of several EHEC/SDS/water systems in sol (—) and gel (---) states. Letters denote the sample type (see Table 1).

establish that the amount of surfactant bound to the polymer is high.

It is also seen in Figure 5 that in the frequency range $350\text{--}950\text{ cm}^{-1}$, which is characteristic for the ring vibrations,²⁵ the spectra of the solutions with and without added surfactant are practically identical, suggesting that the SDS molecules do not interact with or affect the glucose rings (at least at SDS concentrations up to 20 mmol).

Changes during Sol–Gel Transition The temperature scans in Figure 7 show the IR spectral changes of some selected samples upon gelation. The most striking changes are the increase of intensity of the band around 1120 cm^{-1} (C–O–C bridges) and the simultaneous decrease of the band at 1075 cm^{-1} . The increase of the 1120 cm^{-1} band can be explained by a decrease of the mobility of the cellulose rings (see discussion in the “Pure Initial Components” section). On the other hand, the spectral decrease of the band located at 1075 cm^{-1} , assigned to the skeletal vibrations of the rings, involving the C–O ring stretching,^{23,25} also suggests that the rings become less free (or more bound) in the gel state.

A comparison of the Raman spectra for different samples in the sol and gel states is presented in Figure 8. A decrease of the intensity of the band at 1060 cm^{-1} (SO_3^- symmetrical stretch) with gelation is observed for all samples, which indicates that the gelling process affects the sulfonic acid groups. However, since this band does not disappear completely in the gel state, some of the SO_3^- groups are still coordinated with the water molecules when the gel is formed.

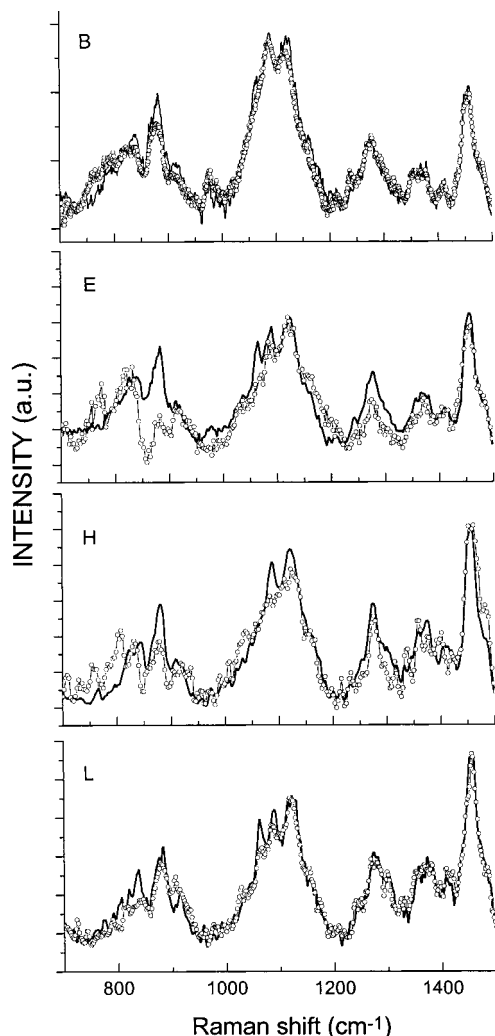


Figure 8. Raman spectra of several EHEC/SDS/water systems in sol (solid line) and gel (open circles) states. Letters denote the sample type (see Table 1).

The most characteristic spectral changes, when going from the sol to the gel state, can be detected in the frequency range corresponding to the glucose ring vibrations ($700\text{--}950\text{ cm}^{-1}$). Although the general spectral profile remains more or less the same, one can observe that with gelation all bands in this region become more distorted, and the center of gravity of the whole spectral envelope shifts toward lower frequencies. Such spectral behavior suggests that the glucose rings are more strongly affected now by the interactions. We note that this is consistent with the present IR results. The changes are dependent on the level of SDS addition, being essentially smaller for samples with high SDS content than for low SDS content samples (compare, e.g., the spectra for the H and L samples in Figure 8). This may be due to the fact that at high surfactant concentrations no temperature-induced gel is formed,^{15,16} and the mobility of SO_3^- groups is only slightly influenced by temperature. At high levels of surfactant addition, the network is disrupted, and the connectivity necessary for the formation of the gel network cannot be reestablished at elevated temperatures.¹⁵

Comparing the changes of the spectra for samples with the same SDS content but with different EHEC concentration (samples B and H), one can see that, despite the same level of SDS addition of both samples (4 mM), the spectrum of sample B shows a behavior

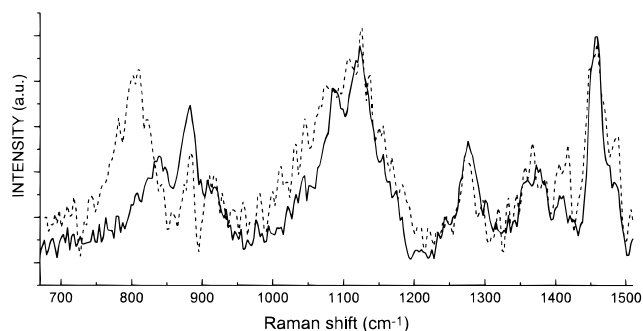


Figure 9. Raman spectra of 2 wt % EHEC aqueous solution at $25\text{ }^{\circ}\text{C}$ (—) and $45\text{ }^{\circ}\text{C}$ (---).

reminiscent of that of the system (sample L) with a high surfactant addition (20 mM). It indicates that the gelation process not only is a function of the absolute surfactant level but also is rather dependent on the SDS-to-EHEC concentration ratio. The finding is supported by the results from a recent oscillatory shear study.¹⁵

To be sure that the spectral variations discussed above are true characteristics of the temperature-induced sol–gel transition in the EHEC–SDS systems, we have also investigated the temperature dependence of the spectra obtained from aqueous EHEC samples without SDS, systems which do not form thermoreversible gels. Figure 9 shows Raman spectra of the sample C (2 wt % EHEC, no SDS) at room and elevated temperatures, and it can be seen that the temperature-induced alterations of the spectrum for the surfactant-free sample have a different character than those for the samples containing SDS. The most striking change is observed in the region $700\text{--}900\text{ cm}^{-1}$, where a new strong band appears at 800 cm^{-1} with raising temperature. In the case of EHEC–SDS systems we noted the general disturbance of the spectral bands in this region with the downward shift of the gravity center (see Figure 8), whereas in the pure EHEC solution the new band becomes dominant in the considered envelope, and its intensity is visibly higher than those of the other bands. It is possible that the prominent spectral change may be associated with the formation of large “lumps”. Indeed, recent small-angle neutron scattering experiments¹⁷ have revealed the formation of large polymer “lumps” in the EHEC/water systems at elevated temperature which increase in size with raising temperature.

We have also investigated during gelation the behavior of water which plays an important role in the polymer–surfactant interaction. Figure 10 displays Raman spectra of the different samples in the sol and the gel states in the frequency region of the HOH bending vibrations. It is seen from the spectra that the relative intensity of the H_2O bending vibrations is lower in the gel state than in the corresponding solution, which shows that the strength of the hydrogen bonds rises upon gelation. Indeed, it is well-known that the oscillator strength of the HOH bending mode decreases rapidly with increasing H-bond strength^{32–34} (for instance, through the series vapor, liquid, amorphous ice, crystalline ice). Thus, the decrease of the band intensity was observed upon aggregation of water molecules,³² with lowering of the temperature of the amorphous ice,³³ or upon the transition from amorphous to cubic ice.³⁴ It

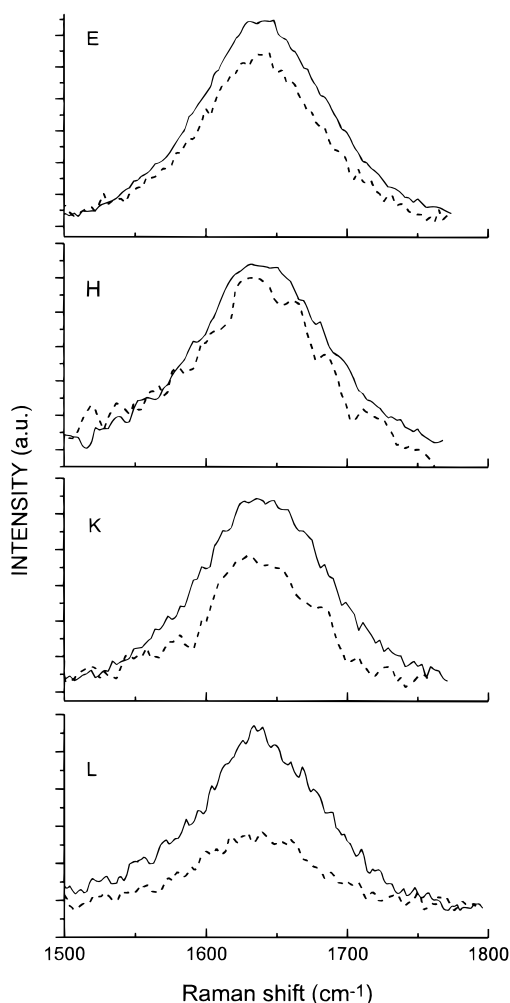


Figure 10. Raman spectra of several EHEC/SDS/water systems in sol (—) and gel (---) states in the frequency region of HOH bending vibration. Letters denote the sample type (see Table 1).

is also seen from Figure 10 that degree of the H-bond strengthening is proportional to the level of the SDS addition (compare samples H and L).

The findings discussed above suggest that at low SDS concentrations the intermolecular interaction is mainly of “SO₃–glucosidic ring” character, whereas at higher concentrations it is better described by an interaction of the “SO₃–water–SO₃” type. This is consistent with the general view on the gelation process,^{15,16} namely, that at low levels of surfactant addition the surfactant is bound to the polymer chains, while at high surfactant concentrations the polymer is “saturated” with the surfactant and surfactant micelles are formed in the solution outside the polymer chains.

Conclusions

From the results of the present Raman and IR studies and from previous findings reported from other experimental techniques, the following picture emerges:

(i) There is an interaction between EHEC and SDS even at temperatures below the gel point, i.e., in the solution state, though the effect is weak and can hardly be characterized as a chemical interaction. SDS interacts mostly with the side chains of the EHEC molecules, and it does not seriously affect the cellulose rings. It is also possible that some of the SO₃ groups of SDS interact with the EHEC molecules.

(ii) When the temperature rises, a new type of interaction appears in the system that may be associated with enhanced chain mobility. The most prominent one is the interaction between the SO₃ groups of SDS and the glucose rings, which leads to an essential decrease of the mobility of the rings and also to their deformations. We have found that this interaction depends on the SDS concentration and that the SDS-to-EHEC concentration ratio plays an important role. The strength of the “SO₃–glucose rings” interaction seems weaker with rising SDS concentration. This can be explained by self-organization of the SO₃ groups via the water molecules. In other words, when the concentration of SO₃ groups is high enough, they start to associate with each other. It means, in turn, that relative interaction of these groups with the EHEC rings will decrease with increasing polymer concentration.

(iii) Clear changes in the state of water occur with gelation. In the gel state the hydrogen bonds between water molecules become stronger. Moreover, the degree of H-bond strengthening increases with the level of SDS addition, which suggests that this effect is inspired by the SO₃[−] groups.

The role of water in the polymer–surfactant interaction is still not clear, especially during the transition from sol to gel. As pointed out above, we found that the Raman spectra show changes in the state of water with gelation, though the behavior needs to be further investigated.

Another issue that is not discussed in this work is the participation of the sodium ion in the interactions. It is obvious (from a general point of view) that Na⁺ takes part at least in the SO₃–water coordination. In principle, there are two ways to clarify this question. First, one can use the set of surfactants with different cations (i.e., for example lithium or potassium DS, etc.) in order to separate out the spectral features characteristic for the processes involving metal ions. Second, one may use other experimental techniques such as NMR which allow to test the local coordination of the cations. However, due to the low surfactant concentrations in real systems, it will be extremely difficult to detect any spectral evidence related to this issue.

References and Notes

- (1) *Microdomains in Polymer Solutions*; Dubin, P., Ed.; Plenum Press: New York, 1985.
- (2) *Interactions of Surfactants with Polymers and Proteins*; Goddard, E. D., Ananthapadmanabhan, K. P., Eds.; CRC Press: Boca Raton, FL, 1993.
- (3) Tanaka, R.; Meadows, J.; Phillips, G. O.; Williams, P. A. *Carbohydr. Polym.* **1990**, *12*, 443.
- (4) Goddard, E. D. *Colloids Surf.* **1986**, *19*, 255.
- (5) Nagarajan, R. *Adv. Colloid Interface Sci.* **1986**, *26*, 205.
- (6) de Gennes, P.-G. *J. Phys. Chem.* **1990**, *94*, 8407.
- (7) Carlsson, A.; Karlstrom, G.; Linndman, B. *J. Phys. Chem.* **1989**, *93*, 3673.
- (8) Karlstrom, G.; Carlsson, A.; Linndman, B. *J. Phys. Chem.* **1990**, *94*, 5005.
- (9) Walderhaug, H.; Nyström, B.; Hansen, F. K.; Lindman, B. *J. Phys. Chem.* **1995**, *99*, 4672.
- (10) Zana, R.; Binana-Limbele; Kamenka, N.; Linndman, B. *J. Phys. Chem.* **1992**, *96*, 5461.
- (11) Kamenka, N.; Burgaud, I.; Zana, R.; Linndman, B. *J. Phys. Chem.* **1994**, *98*, 6785.
- (12) Carlsson, A.; Karlstrom, G.; Linndman, B. *Colloids Surf.* **1990**, *47*, 147.
- (13) Nyström, B.; Lindman, B. *Macromolecules* **1995**, *28*, 967.
- (14) Nyström, B.; Roots, J.; Carlsson, A.; Linndman, B. *Polymer* **1992**, *33*, 2875.
- (15) Kjoniksen, A.-L.; Nyström, B.; Lindman, B. *Macromolecules* **1998**, *31*, 1852.

- (16) Nyström, B.; Kjoniksen, A.-L.; Lindman, B. *Langmuir* **1996**, *12*, 3233.
- (17) Cabane, B.; Lindell, K.; Engström, S.; Lindman, B. *Macromolecules* **1996**, *29*, 3188.
- (18) Holmberg, C. *Colloid Polym. Sci.* **1996**, *274*, 836.
- (19) Nahringsbauer, I. *Langmuir* **1997**, *13*, 2242.
- (20) Tanaka, F. *Macromolecules* **1998**, *31*, 384.
- (21) Semenov, A. N.; Rubinstein, M. *Macromolecules* **1998**, *31*, 1373.
- (22) Semenov, A. N.; Rubinstein, M. *Macromolecules* **1998**, *31*, 1386.
- (23) Cael, J. J.; Gardner, K. H.; Koenig, J. L.; Blackwell, J. J. *J. Chem. Phys.* **1975**, *62*, 1145.
- (24) Zhbankov, R. G. *J. Mol. Struct.* **1992**, *272*, 347.
- (25) Edwards, H. G. M.; Farwell, D. W.; Williams, A. C. *Spectrochim. Acta* **1994**, *50A*, 807.
- (26) Kondo, T.; Sawatari, C. *Polymer* **1996**, *37*, 393.
- (27) Ivanova, N. V.; Korolik, E. V.; Zhbankov, R. G.; Insarova, N. I. *J. Appl. Spectrosc.* **1989**, *49*, 301.
- (28) Dehant, I.; Danc, R.; Kimmer, V.; Shmolke, R. *Infrared Spectroscopy of Polymers*.
- (29) Sivchik, V. V.; Zhbankov, R. G. *J. Appl. Spectrosc.* **1977**, *27*, 853.
- (30) Panov, V. P.; Zhbankov, R. G. *Intra- and Intermolecular Interactions in Carbohydrates* (in Russian); Minsk: Moscow, 1988.
- (31) ATLAS.
- (32) Pimentel, G. C.; McClellan A. L. In *The Hydrogen Bond*; Freeman: San Francisco, CA, 1960; p 120.
- (33) Devlin, J. P.; Wooldridge, P. J.; Ritzhaupt, J. J. *J. Chem. Phys.* **1986**, *84*, 6095.
- (34) Devlin, J. P. *J. Mol. Struct.* **1990**, *224*, 33.

MA9814191